Bioorganic Chemistry 87 (2019) 679–687

Contents lists available at ScienceDirect

Bioorganic Chemistry

journal homepage: www.elsevier.com/locate/bioorg

5-Thioxoimidazolidine-2-one derivatives: Synthesis, anti-inflammatory activity, analgesic activity, COX inhibition assay and molecular modelling study

Marwa A.M.Sh. El-Sharief[a,b,*], Samir Y. Abbas[c,*], Ahmed M.Sh. El-Sharief[d], Nermien M. Sabry[a], Ziad Moussa[e], Shahenda M. El-Messery[f], Ahmed R. Elsheakh[g], Ghada S. Hassan[h,*], Mardia T. El Sayed[a]

[a] Applied Organic Chemistry Department, National Research Centre, Cairo, Egypt
[b] Faculty of Science and Arts, Mohail Asser, King Khalid University, Saudi Arabia
[c] Organometallic and Organometalloid Chemistry Department, National Research Centre, Cairo, Egypt
[d] Chemistry Department, Faculty of Science, Al-Azhar University (Boys), Cairo, Egypt
[e] Department of Chemistry, College of Science, United Arab Emirates University, P.O. Box 15551, Al-Ain, United Arab Emirates
[f] Department of Pharmaceutical Organic Chemistry, Faculty of Pharmacy, Mansoura University, Mansoura, Egypt
[g] Department of Pharmacology and Toxicology, Faculty of Pharmacy, Mansoura University, Mansoura, Egypt
[h] Department of Medicinal Chemistry, Faculty of Pharmacy, Mansoura University, Mansoura, Egypt

ARTICLE INFO

Keywords:
N-Arylcyanothioformamides
Imidazolidineiminothiones
Imidazolidin-2,5-diones
Anti-inflammatory activity
Analgesic activity
COX inhibition assay

ABSTRACT

A series of 5-imino-4-thioxo-2-imidazolidinone derivatives with different substituents at N^1 and N^3 was synthesized with high yield and excellent purity by the reaction of different *N*-arylcyanothioformamide derivatives with isocyanate derivatives. Treatment 5-imino-4-thioxo-2-imidazolidinone derivatives with acidic medium afforded 4-thioxoimidazolidin-2,5-dione derivatives. The structures of the obtained products were established based on spectroscopic IR, ^{1}H NMR, ^{13}C NMR, ^{1}H, ^{1}H-COSY, HSQC and elemental analyses. The anti-inflammatory activity of the synthesized compounds through the carrageenan-paw edema model as well as *in vitro* COX-1 and COX-2 inhibition assay were evaluated where most of the synthesized compounds showed significant anti-inflammatory activity. Mostly, all of our synthesized compounds have greater activity more than celecoxib toward both cyclooxygenase enzymes. All of the tested compounds (except one compound) exhibited IC_{50} valves for COX-2 ranged from 0.001×10^{-3} to 0.827×10^{-3} μM while the reference drug has IC_{50} 40.0×10^{-3} μM. Furthermore, the analgesic activity of such compounds was also determined. Molecular modeling study was also conducted to rationalize the potential as anti-inflammatory agents of our synthesized compounds by predicting their binding modes, binding affinities and optimal orientation at the active site of the COX enzymes.

1. Introduction

Inflammation is one of the immune response of the body to microbe's infections and injury as well as it is key to autoimmune diseases, such as multiple sclerosis, rheumatoid arthritis, Crohn's disease and type I diabetes [1–4]. The generation of prostaglandins is one of the most important factors in the inflammatory process, they are produced within the body's cells by the cyclooxygenase (Cox) enzyme. Both Cox-1 and Cox-2 enzymes produce prostaglandins that promote inflammation, pain and fever. Nonsteroidal anti-inflammatory drugs are drugs with analgesic and antipyretic (fever-reducing) effects and which have, in higher doses, anti-inflammatory effects. Nonsteroidal anti-inflammatory drugs block the Cox enzymes and reduce prostaglandins throughout the body. As a consequence, ongoing inflammation, pain and fever are reduced. Since the prostaglandins that protect the stomach and support the platelets and blood clotting also are reduced. So, there is need for discover safe and effective anti-inflammatory compounds [5–10]. The imidazole moiety is one of the most important synthetic strategies in drug discovery. Imidazole derivatives have broadened scope in clinical medicines such as anti-inflammatory, antidiabetic, anticoagulants, anticancer, antibacterial, antifungal, antiviral, antitubercular and antimalarial activities [11–13]. Imidazole nucleus incorporated in the several natural products structures such as histidine (essential amino-acid), metronidazole (anti-parasitic),

* Correspondence authors at: Applied Organic Chemistry Department, National Research Centre, Cairo, Egypt (M.A.M.Sh. El-Sharief).
E-mail addresses: mrwa1976@hotmail.com (M.A.M.S. El-Sharief), samiryoussef98@yahoo.com (S.Y. Abbas), ghadasameh@mans.edu.eg (G.S. Hassan).

https://doi.org/10.1016/j.bioorg.2019.03.075
Received 7 December 2018; Received in revised form 8 March 2019; Accepted 30 March 2019
Available online 01 April 2019

cimetidine (antihistaminic), dacarbazine (anti-tumoral, anti-cancer) and losartan (antihypertensive) [14,15]. Imidazolidineiminothiones and the various heterocycles derived from them were shown to exhibit an interesting and a wide range of pharmacological effects against antitumor, antiviral, antibacterial and antifungal strains [16–20]. As far as, we aware imidazolidineiminothione and 4-thioxoimidazolidin-2,5-dione derivatives are did not investigated as anti-inflammatory or analgesic agents. In light of these facts, the present study was designed to synthesize new imidazolinone derivatives and evaluate their anti-inflammatory activity. As a trial to obtain novel class of anti-inflammatory agents, different groups were introduced into the target compounds with the aim of finding new and more potent anti-inflammatory agents. Moreover, considering that computer docking techniques play an important role in mechanistic studies by placing a molecule into the binding site of the target macromolecule in a non covalent fashion, we have docked our compounds into the active site of COX-1 and COX-2 enzymes. Our objective is to rationalize the potential as anti-inflammatory agents of these compounds by predicting their binding modes, binding affinities and optimal orientation at the active site of the COX-1 and COX-2 enzymes.

2. Results and discussion

2.1. Chemistry

The aim of the present investigation is to synthesize a series of imidazolidineiminothiones which bearing different substituent at N-(1) and others at N-(3).

The synthetic strategy of the target compounds was illustrated in Scheme 1 where *N*-arylcyanothioformamide derivatives **1a-c** were prepared by the reaction of arylisothiocyanates with potassium cyanide according to the reported procedure [16]. The reactions of **1a-c** with different isocyanate derivatives in ether, in presence of catalytic amount of triethylamine were carried out to afford imidazolidineiminothione derivatives **2a-i**. The 5-imino-4-thioxo-2-imidazolidinone derivatives **2a-i** were furnished as the sole products, indicating that the ring closing reaction proceeds *via* a single path which involves attack *via* the nitrogen atom. Hydrolysis of 5-imino-4-thioxo-2-imidazolidinone derivatives **2a-i** with dilute HCl in boiling ethanol proceed the target Imidazolidin-2,5-dione derivatives **3a-i**.

2.1.1. IR spectral analysis

The IR spectra of imidazolidineiminothione derivatives **2a-i** showed bands in 3460–3430 cm^{-1} region for the imino NH functional group, 1780–1771 cm^{-1} for the C=O functional group, and 1670–1665 cm^{-1} for the C=N functional group. IR spectrum of **2a**, as representative example, showed bands at 3460, 1780, 1670 and 1128 cm^{-1} for NH, C=O, C=N and C=S functional groups, respectively. Moreover, IR spectra of imidazolidin-2,5-dione derivatives **3a-i** showed disappearance of bands for NH and C=N functional groups. IR spectrum of **3a**, as representative example, exhibited characteristic bands at 1748 and 1120 cm^{-1} for C=O and C=S functional groups, respectively (See Supplementary Data).

2.1.2. ^{1}H NMR spectral analysis

The ^{1}H NMR spectrum of compound **2g**, as representative example, was characterized by the presence of triplet and quartet signals at: δ = 1.44 and 4.08 ppm corresponding for ethoxy protons. Also, a singlet signal at 2.40 ppm was observed for the methyl protons. Beside the latter three aliphatic signals, the ^{1}H NMR spectrum of compound **2g** exhibited four douplet signals for AB aromatic protons at: 7.02, 7.32, 7.37 and 7.43 ppm with two proton integral value which are assigned to protons at C-2,6 and C-3,5 carbons of ethoxyphenyl and *p*-tolyl moieties. The broad exchangeable signal at 9.52 ppm is assigned for the imine proton. ^{1}H, ^{1}HCOSY spectra of all of the synthesized imidazole derivatives supported these assignments (See Supplementary Data).

2.1.3. ^{1}H, ^{1}H-COSY spectral analysis

^{1}H, ^{1}H-COSY supported the interpretations of structures elucidation of all the obtained products. ^{1}H, ^{1}H-COSY-COSY of compound **2g**, as representative example, revealed the following information. Methyl protons do not coupled with any other protons. The two groups of ethoxy protons are coupled with each other only and do not coupled with any other protons. Each of the two protons at C-2,3 and C-5,6 carbons of ethoxyphenyl and *p*-tolyl moieties are *ortho*-coupled with each other. The *meta*-coupling of the protons at C-2 and C-3 carbons of ethoxyphenyl and *p*-tolyl moieties with the protons at C-6 and C-5 carbons of ethoxyphenyl and *p*-tolyl moieties, respectively, were not observed (See Supplementary Data).

2.1.4. ^{13}C NMR spectral analysis

^{13}C NMR (on-resonance & DEPT) spectral assignment of all the obtained products has been made. ^{13}C NMR spectra of **2a-i** displayed the expected three signals for the 4-imino-5- thioxoimidazolidine-2-one core at 153.8–154.1 ppm for C=N, 154.0–154.5 ppm for C=O and 181.3–181.8 ppm for C=S. In general, the aromatic carbons could be readily distinguished from the other carbons due to their characteristic absorption. ^{13}C NMR spectrum of compound **2g**, as representative example, showed three signals in the aliphatic region. The signals at 14.7, 21.2, and 63.8 ppm are due to $\underline{CH_3}CH_2$, CH_3 and CH_2 carbons,

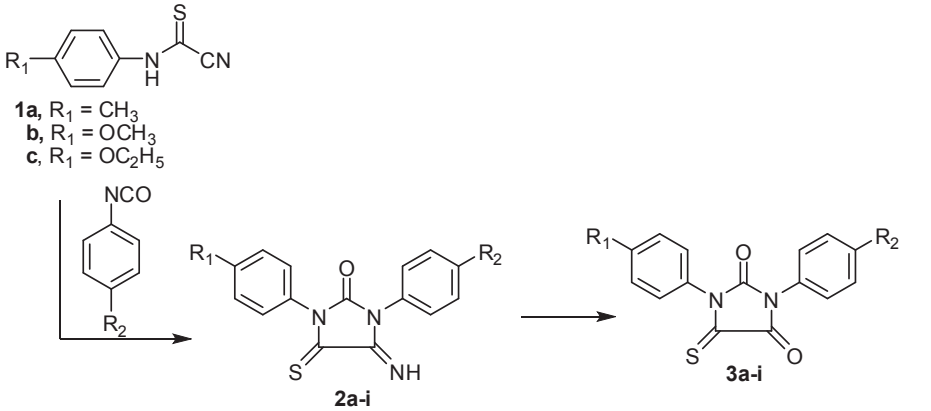

Scheme 1. Synthesis of the target imidazolidineiminothione derivatives **2a-i** and imidazolidin-2,5-dione derivatives **3a-i**.

respectively. The signals resonated at: 115.1, 126.3, 128.3 and 130.0 ppm are assigned to 8CH carbons, while the signals resonated at: 125.1, 129.4, 138.7 and 159.6 ppm are assigned to 4C carbons. The signals resonated in the deshielded region at 154.0, 154.4, 181.8 ppm are assigned to C═N, C═O, C═S carbons, respectively. ^{1}H, ^{13}C Heteronuclear Single Quantum Coherence (HSQC) spectra of all the obtained products supported these assignments and added a strong evidence for these interpretations (See Supplementary Data).

2.1.5. ^{1}H, ^{13}C Heteronuclear single Quantum Coherence (HSQC) spectral analysis

From the ^{1}H–^{13}C HSQC spectrum of **2g**, as representative example, the following assignments: Triplet signal at 1.39 ppm showed cross peak with the signal at 14.7 ppm. This suggests that the carbon signal is due to methyl carbon of ethoxy group. Singlet signal at 2.41 ppm showed cross peak with the signal at 21.2 ppm. This suggests that the carbon signal is due to methyl group. Quartet signal at 4.10 ppm showed cross peak with the signal at 63.8 ppm. This suggests that the carbon signal is due to methylene carbon of ethoxy group. The four douplet signals for AB aromatic protons at: 7.02, 7.32, 7.37 and 7.43 ppm which are assigned to protons at C-2,6 and C-3,5 carbons of ethoxyphenyl and *p*-tolyl moieties show cross peak with the signal at 115.1, 126.3, 128.3 and 130.0 ppm. The assignment of NH proton was confirmed as there are no correlations for NH by HSQC spectral analysis. In the HSQC spectrum, there are seven signals without correlations at: 124.4 (C), 127.8 (C), 139.2 (C), 153.0 (C═O), 153.5 (C═O), 159.8 (C−O), 182.7 (C═S) ppm (See Supplementary Data).

2.2. Biological evaluation

2.2.1. Anti-inflammatory activities

To assay anti-inflammatory activity, the paw edema test has been widely employed *via* measuring the ability of the tested compounds to reduce induced edema. So, In order to determine the anti-inflammatory activity of the synthesized compounds in acute-phase inflammation, the newly synthesized compounds were evaluated with a carrageenan-induced rat paw edema bioassay in rats [21,22] using celecoxib as a reference standard. Generally, as shown in Table 1, all of the tested compounds proved to be active as they exhibited inhibition percentage for inflammation ranged from 80.5 to 88.6 which is very closely equal to that produced by the reference drug. A moderate difference in the anti-inflammatory activity is noted between the tested compounds. This suggested that, the main effect may be related to the presence of the imidazolidinethione moiety. Compound **2d** exerted the highest percentage inhibition among all the synthesized compounds with value that equal 88 ± 6.3, followed by compound **3i** (87 ± 3.8 I%).

2.2.2. In vitro cyclooxygenase inhibitory assay

The percentage of inhibition of COX-1 and COX-2 of tested compounds at concentration of 5.0 μM were illustrated in Table 1. In general, all of the tested compounds exhibited high % inhibition values for both COX-1 and COX-2. As shown in Table 1, all of the tested compounds exhibited inhibition percentage for COX-1 ranged from 84.16 (compound **3f)** to 85.95 (compound **2e**). The percentage of inhibition of COX-1 for the tested compounds was observed to be much higher than that of the reference drug where the inhibition percentage of the reference drug (2.20) is very low related to our synthesized compounds. Regard to COX-2, as shown in Table 1, all of the tested compounds exhibited inhibition percentage for COX-2 ranged from 82.50 (compound **2d)** to 87.90 (compound **3i**). The percentage of inhibition of COX-2 for the tested compounds was observed to be much higher than the Celecoxib by about 1.5-fold. The tested compounds revealed the non-selectivity of them toward inhibition of COX-1 or COX-2 where the selectivity Index is near to one for all of the tested compounds.

2.2.3. Determination of the IC_{50} of the target compounds

The IC_{50} for both COX-1 and COX-2 of the synthesized compounds was determined using Cayman colorimetric COX (ovine) inhibitor screening assay [21–23]. Regarding to the COX-1 values, as shown in Table 1, all of the tested compounds exhibited IC_{50} values lower than that of the reference drug, except compound **3f** that has equal value and compound **2f** that has double value of that of celecoxib, otherwise the rest of the compounds had very low values of their IC_{50} especially compound **3g** that has IC_{50} 0.0003 μM while the reference drug has IC_{50} 2.8 μM, So compound **3g** is considered very potent active agent, in addition to compounds **2g, 3e, 2b** and **2d** that has IC_{50} value of 0.0021, 0.0040, 0.0360 and 0.0840 μM, respectively. On the other hand, the IC_{50} of the tested compounds against COX-2 was also determined, all of the synthesized products exhibited very low values reflecting their high potency. All of the tested compounds (except **2a**) exhibited IC_{50} values for COX-2 ranged from 0.001×10^{-3} μM (compound **3e)** to 0.827×10^{-3} μM (compound **3a**) while the reference drug has IC_{50} 40.0×10^{-3} μM. The lowest value was represented by compounds **3e**, **2b, 2h, 3g** and finally **2f** with IC_{50} values of 0.001×10^{-3},

Table 1
The percentage inhibition of COX-1 and COX-2 of the target compounds.

Compd. No.	% inhibition (I%)	%I COX-1[a]	%I COX-2[a]	IC_{50} (μM) (COX-1)	IC_{50} (μM) (COX-2)	Selectivity Index (SI) (COX-2/COX-1)
2a	82 ± 1.8	85.46	83.77	1.4640	11.800×10^{-3}	8.06×10^{-3}
2b	82 ± 5.0	85.87	85.65	0.0360	0.002×10^{-3}	5.56×10^{-5}
2c	83 ± 7.4	85.07	82.59	1.9310	0.205×10^{-3}	1.06×10^{-4}
2d	88 ± 6.3	85.81	82.50	0.0840	0.582×10^{-3}	6.93×10^{-3}
2e	84 ± 7.4	85.95	82.83	0.4636	0.463×10^{-3}	9.98×10^{-4}
2f	82 ± 4.4	85.46	85.52	5.2661	0.005×10^{-3}	9.49×10^{-7}
2g	84 ± 2.9	85.89	84.16	0.0021	0.372×10^{-3}	0.1771
2h	85 ± 3.6	85.36	84.76	0.8551	0.002×10^{-3}	2.34×10^{-6}
2i	86 ± 3.7	85.90	84.20	0.1600	0.067×10^{-3}	4.18×10^{-4}
3a	80 ± 2.4	84.96	84.39	0.7610	0.827×10^{-3}	1.09×10^{-3}
3b	83 ± 7.3	85.25	85.29	0.1320	0.220×10^{-3}	1.67×10^{-3}
3c	84 ± 9.1	85.85	83.89	0.3112	0.527×10^{-3}	1.69×10^{-3}
3d	81 ± 2.7	85.72	85.19	1.1064	0.023×10^{-3}	2.09×10^{-5}
3e	83 ± 4.6	85.72	85.35	0.0040	0.001×10^{-3}	2.5×10^{-4}
3f	79 ± 8.1	84.16	85.01	2.8570	0.120×10^{-3}	4.17×10^{-5}
3g	85 ± 5.8	85.78	84.04	0.0003	0.002×10^{-3}	6.67×10^{-3}
3h	82 ± 7.4	85.52	83.74	1.8950	0.286×10^{-3}	1.51×10^{-4}
3i	87 ± 3.8	84.91	87.90	0.9453	0.387×10^{-3}	4.09×10^{-4}
Celecoxib	89 ± 1.6	2.20	61.40	2.8000	40.00	0.014

[a] Values represents means of two determinations acquired using an ovine COX-1/COX-2 assay kits.

Table 2
The analgesic activity (ED_{50} μM/Kg) of the tested compounds.

Compound No.	(ED_{50} μM/Kg)		
	0.5 h	1.0 h	2.0 h
2a	78 ± 2.4	115 ± 4.9	117 ± 3.6
2b	69 ± 5.1	122 ± 7.4	123 ± 2.2
2c	81 ± 3.0	137 ± 9.4	134 ± 3.8
2d	93 ± 4.9	119 ± 5.6	122 ± 7.7
2e	77 ± 6.1	148 ± 2.5	149 ± 6.0
2f	89 ± 2.8	139 ± 8.4	137 ± 5.2
2g	68 ± 7.4	127 ± 6.1	127 ± 8.7
2h	63 ± 4.2	153 ± 5.2	155 ± 4.3
2i	79 ± 3.9	144 ± 1.3	149 ± 7.3
3a	86 ± 8.4	149 ± 5.0	155 ± 3.7
3b	89 ± 2.9	173 ± 2.1	178 ± 2.6
3c	92 ± 9.3	183 ± 5.5	181 ± 7.4
3d	95 ± 5.5	194 ± 7.6	201 ± 4.5
3e	73 ± 7.2	171 ± 8.4	175 ± 3.4
3f	68 ± 2.3	164 ± 9.7	160 ± 9.1
3g	70 ± 1.1	151 ± 8.2	155 ± 9.8
3h	72 ± 3.4	149 ± 5.2	155 ± 3.9
3i	80 ± 2.9	173 ± 8.2	179 ± 2.1
Celecoxib	159 ± 4.7	75.2 ± 1.4	70 ± 3.9

0.002×10^{-3}, 0.002×10^{-3}, 0.002×10^{-3} and 0.005×10^{-3} μM, respectively. So these compounds are considered very potent anti-inflammatory agents. The selectivity index (SI) for the synthesized compounds was calculated by dividing the IC_{50} against COX-2 by the IC_{50} against COX-1 of the same compound. These values were obtained for the evaluation of the selectivity of the target compounds against COX-2. According to this concept, the lower value of the SI mean the higher the selectivity of the compound against COX-2. The results revealed that compounds **2f** and **2h** proved to be the most selective ones towards COX-2 with SI value of 9.49×10^{-7} and 2.34×10^{-6}, respectively; compound **2b, 3d** and **3f** were of lower selectivity with SI values of 5.56×10^{-5}, 2.09×10^{-5} and 4.17×10^{-5} respectively. On the other hand, the SI value of compound **2g** is the least among the other target compounds it has value of 0.1771 which represents about one tenth of the SI value of the standard compound Celecoxib (SI value = 0.014).

2.2.4. Determination of analgesic activity

The analgesic activity of the synthesized compounds were determined and illustrated in Table 2, from the showing data, it was revealed that after 1 and 2 h of administration of compounds, all of the tested compounds showed significant analgesic activity higher than that obtained by celecoxib. After 1 h of administration, all of the tested compounds exhibited ED_{50} valves ranged from 115 μM (compound **2a)** to 194 μM (compound **3d**) while the reference drug has ED_{50} 75.2 μM. Moreover, after 2 h of administration, all of the tested compounds exhibited ED_{50} valves ranged from 117 μM (compound **2a)** to 201 μM (compound **3d**) while the reference drug has ED_{50} 70 μM. Mostly, the tested compounds exhibited significant analgesic activity ranged from twofold to threefold compare to the reference drug. Compound **3d** exhibited nearly threefold analgesic effect to reference drug. So these compounds are considered very potent analgesic agents.

Table 3
Binding energies of selected compounds with COX-1 and COX-2 (kcal/mol).

Compound No.	Binding energy COX-1 kcal/mol	Binding energy COX-2 kcal/mol
2b	−11.41128	−13.99606
3e	−12.04081	−12.82521
3g	−12.83963	−13.85701
Celecoxib	−14.30098	−15.42995

2.2.5. Molecular modelling

Our objective is to rationalize the potential of the synthesized compounds as anti-inflammatory agents by predicting their binding modes, binding affinities and optimal orientation at the active site of the COX enzymes. The molecular modeling studies were performed with the MOE software program. It is known that the main difference between the two COX active sites is the replacement of Ile 523 in COX-1 by Val 523, a less bulky amino acid. This replacement causes COX-2 binding site 25% larger than the COX-1 and creates an adjunct pocket in the COX-2 active site which may be responsible for selectivity [24,25]. While our results have further shows that inhibitors of COX-1 can equally inhibit COX-2, thus assuming equipotency, and this could be interpretated by assuming that these ligands could takes an alternative mode of orientation from the original reference through interaction with the active site. The least energy conformers of selected compounds **2b, 3e** and **3g** were illustrated in Fig. 1.

The 2D and 3D binding models of compounds **2b, 3e** and **3g** into both crystal structures of COX-1 and COX-2 were depicted in comparison to celecoxib reference. Their binding energies were illustrated in Table 3.

Starting with COX-1, the binding of celecoxib with COX-1 is considered to be a complex interaction *via* Leu 352, Glu 192, Phe 518 and Ser516 hydrogen bonding network resulting in tight binding. (Fig. **2. 1**). Docking results also had showed that compound **2b** (IC_{50} 0.0360 μM) could bind into the same active site of COX-1 as celecoxib with a binary hydrogen bonding interaction with Ile 523 and Ser530 which seems to be of higher importance for activity Fig. 2**. 2**.

Compound **3e** (IC_{50} 0.004 μM) was docked into the active site of COX-1 and the interaction energy of 12.04081 kcal/mol was obtained. Two hydrogen bonding interaction between methoxy oxygen of **3e** with both Ser530 and Ser516 of COX-1 active site was observed (Fig. 3**. 1**). In addition to occupying the active site which was easily illustrated *via* drawing surface map (Fig. 3**. 2**).

Moreover compound **3g** (IC_{50} 0.0003 μM) also binds with COX-1 active site through its ethoxy oxygen *via* a binary hydrogen bonding interaction with both Ser516 and His90 (Fig. 4. 1). Compound **3g** was located deeply inside the pocket (Fig. 4**. 2**).

The molecular docking of celecoxib as a reference into COX-2 isoenzyme was obtained. As shown in Fig. 5**. 1**, it binds to the following amoinoacids by a network of hydrogen bonding with Leu338, Ser339, Gln178, His75 and Tyr 341. As shown in Fig. 5**. 2** compound **2b** (IC_{50} 0.002×10^{-3} μM) into binding site of COX-2 showed interact by a favorable hydrogen bonding interaction with Tyr 341 in addition to phenyl ring with Arg499. As shown in Fig. 5**. 3**, phenyl ring seems in

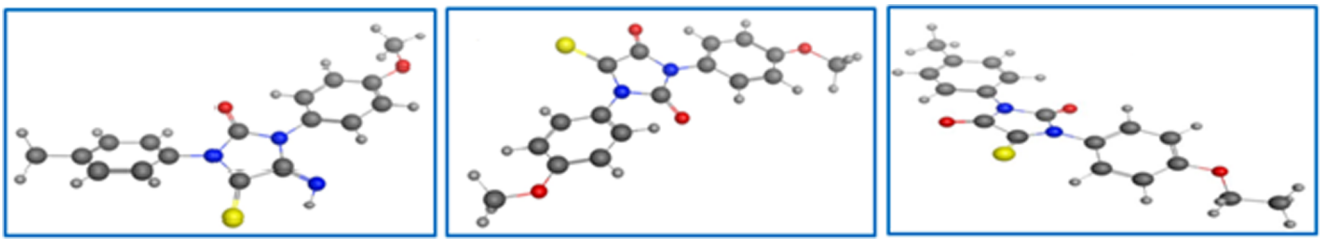

Fig. 1. Lowest energy conformers of some selected active compounds**. 1.1: 2b, 1.2: 3e** and **1.3: 3g** with balls and cylinders rendering.

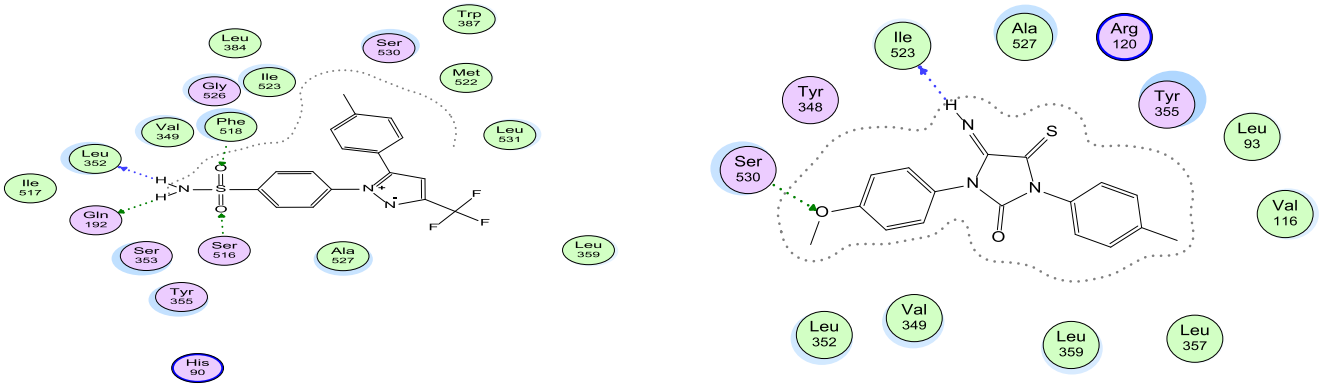

2.1. 2.2.

Fig. 2. 2.1.: 2D binding mode and residues involved in the recognition of celecoxib reference, **2.2**: Compound **2b** docked and minimized in the COX 1 binding pocket.

the construction site is important for increasing COX-2 inhibition.

As shown in Fig. 6. 1., compound **3e** firstly interacted with Arg106 in the side pocket of COX-2 through its phenyl moiety then reorients in the active site so that the methoxy moiety forms hydrogen bond with Ser516 in the active site. In addition; as shown in Fig. 6**. 1** compound **3g** (IC_{50} 0.002×10^{-3} μM) interaction forces the carbonyl core to adopt a specific orientation at the top of the channel causing binding with both critical amino acids Try341 and Ser516, occupying the active site nicely and efficiently Fig. 6**. 2 and 6.3**.

3. Conclusion

New series of Imidazolidineiminothione and Imidazolidin-2,5-dione derivatives were synthesized and evaluated for for anti-inflammatory and analgesic activities. The anti-inflammatory activity was conducted, the results revealed that all the tested compounds exhibited high activity when compared with the reference drug. Generally, all of the tested compounds proved to be active as they exhibited inhibition percentage for inflammation ranged from 80.5 to 88.6 which is very closely equal to that produced by the reference drug. A moderate difference in the anti-inflammatory activity is noted between the tested compounds. This suggested that, the main effect may be related to the presence of the imidazolidinethione moiety. Compound **2d** exerted the highest percentage inhibition among all the synthesized compounds with value that equal 88 ± 6.3, followed by compound **3i** (87 ± 3.8 I %). Mostly, all of our synthesized compounds have shown greater activity even more than reference compound celecoxib in both cyclooxygenase forms. All of the tested compounds (except one compound) exhibited IC_{50} valves for COX-2 ranged from 0.001 to 0.827×10^{-3} μM while the reference drug has IC_{50} 40.0×10^{-3} μM. So, these compounds are considered very potent anti-inflammatory agents. The analgesic activity was also studied. Mostly, the tested compounds exhibited significant analgesic activity ranged from twofold to threefold compare to the reference drug. Compound **3d** exhibited nearly threefold analgesic effect to reference drug. So these compounds are considered very potent analgesic agents.

4. Experimental section

IR spectra were recorded (KBr) on a Perkin Elmer 1650 spectrophotometer. ^{1}H NMR and ^{13}C NMR spectra were recorded on Avance II Bruker FT NMR spectrometer 400 (400 MHz) using $CDCl_3$ as solvents and TMS as an internal standard. Chemical shifts are expressed as δ ppm units. Melting points were obtained on a Fishere Johns melting points apparatus and are uncorrected.

4.1. General procedure for the synthesis of imidazolidineiminothione derivatives 2a-i

A solution of the cyanothioformanilide derivatives **1a-c** (0.01 mol) with the corresponding isocyanate derivatives (0.01 mol) in dry ether (30 mL) and in presence of catalytic amount of triethyl amine was stirred for 15 min at room temperature. The solid obtained was filtered off, washed with ether, air-dried and recrystallized from chloroform/*n*-hexane to give target derivatives **2a-i**.

4.1.1. 4-Imino-5-thioxo-1,3-di-p-tolylimidazolidin-2-one (2a)

Yield 79%; m.p. 177–178 °C; IR: ν/cm^{-1}: 3460 (NH), 1780 (C═O),

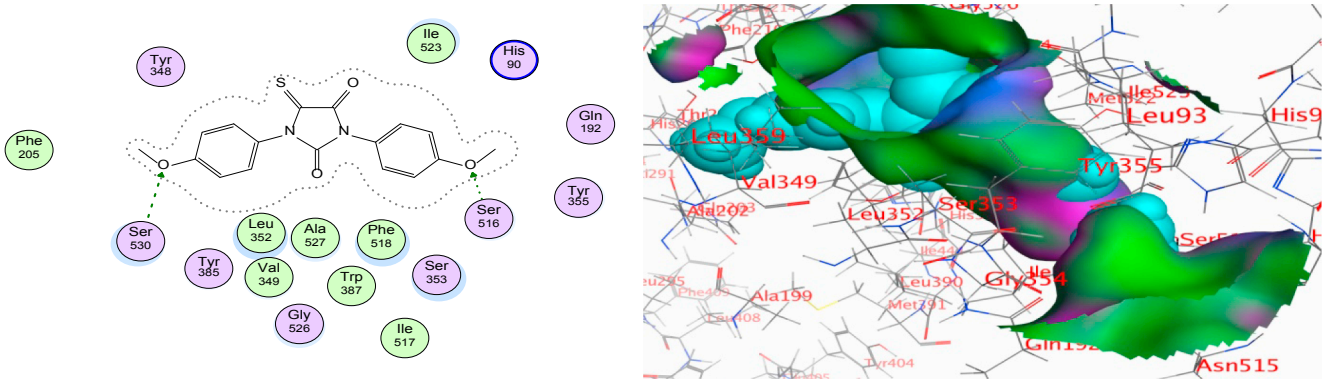

3.1. 3.2.

Fig. 3. 3.1: 2D binding mode and residues involved in the recognition of compound **3e**, **3.2**: The aligned conformation of compound **3e** (space filled cyan) occupying COX1 binding pocket.

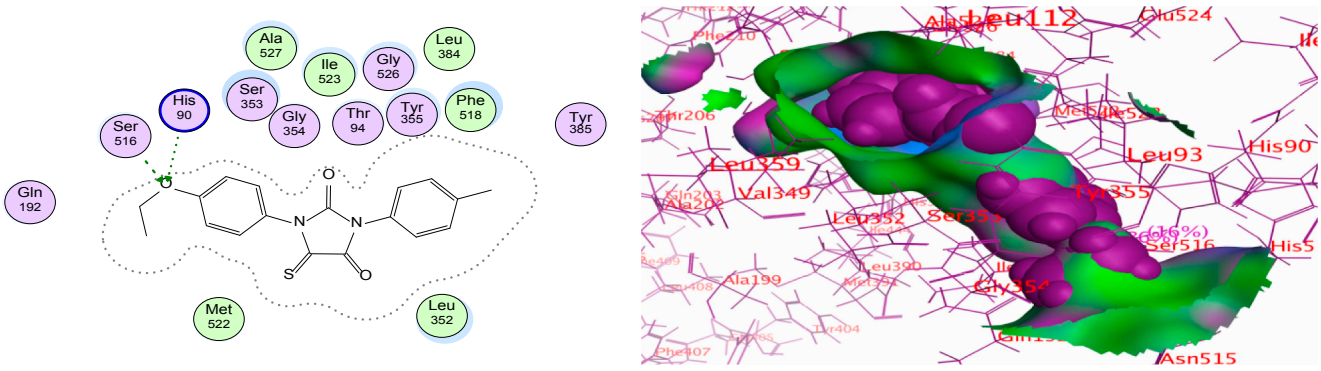

4.1 **4.2**

Fig. 4. 4.1: 2D binding mode and residues involved in the recognition of compound **3g**, **4.2**: The aligned conformation of the most active compound **3g** (space filled violet) occupying COX1 binding pocket.

1670 (C═N), 1128 (C═S); ^{1}H NMR ($CDCl_3$, 400 MHz) δ/ppm = 2.40 (s, 3H, CH_3), 2.42 (s, 3H, CH_3), 7.32 (d, 2H, *J* = 8.4 Hz, Ar-H), 7.35–7.33 (m, 4H, Ar-H), 7.43 (d, 2H, *J* = 8.4 Hz, Ar-H), 9.52 (br, 1H, NH); ^{13}C NMR ($CDCl_3$, 100 MHz): 21.2 (CH_3), 21.3 (CH_3), 126.3 (2CH), 126.8 (2CH), 129.3 (C), 129.9 (2CH), 130.1 (2CH), 130.2 (C), 138.7 (C), 139.9 (C), 153.9 (C═N), 154.0 (C═O), 181.7 (C═S); Anal. calcd for $C_{17}H_{15}N_3OS$ (309.39): C, 66.00; H, 4.89; N, 13.58; Found: C, 66.14; H, 4.87; N, 13.63%

4.1.2. 4-Imino-3-(4-methoxyphenyl)-5-thioxo-1-(p-tolyl)imidazolidin-2-one (2b)

Yield 85%; m.p. 120–121 °C; IR: ν/cm^{-1}: 3439 (NH), 1775 (C═O), 1666 (C═N), 1250 (C–O), 1175 (C–O), 1125 (C═S); ^{1}H NMR ($CDCl_3$, 400 MHz) δ/ppm = 2.43 (s, 3H, CH_3), 3.84 (s, 3H, OCH_3), 7.03 (d, 2H, *J* = 9.1 Hz, Ar-H), 7.36–7.33 (m, 4H, Ar-H), 7.46 (d, 2H, *J* = 9.1 Hz, Ar-H), 9.50 (s, 1H, NH); ^{13}C NMR ($CDCl_3$, 100 MHz): 21.3 (CH_3), 55.5 (CH_3), 114.7 (2CH), 124.5 (C), 126.8 (2CH), 127.9 (2CH), 130.1 (2CH), 130.2 (C), 139.9 (C), 154.0 (C═N), 154.5 (C═O), 159.5 (C–O), 181.8 (C═S); Anal. calcd for $C_{17}H_{15}N_3O_2S$ (325.38): C, 62.75; H, 4.65; N, 12.91; Found: C, 62.81; H, 4.61; N, 12.87%.

4.1.3. 4-Imino-3-(4-(methylthio)phenyl)-5-thioxo-1-(p-tolyl)imidazolidin-2-one (2c)

Yield 80%; m.p. 110–112 °C; IR: ν/cm^{-1}: 3451 (NH), 1777 (C═O), 1665 (C═N), 1092 (C═S);^{1}H NMR ($CDCl_3$, 400 MHz) δ/ppm = 2.43 (s, 3H, CH_3); 2.51 (s, 3H, SCH_3), 7.36–7.33 (m, 4H, Ar-H), 7.38 (d, 2H,

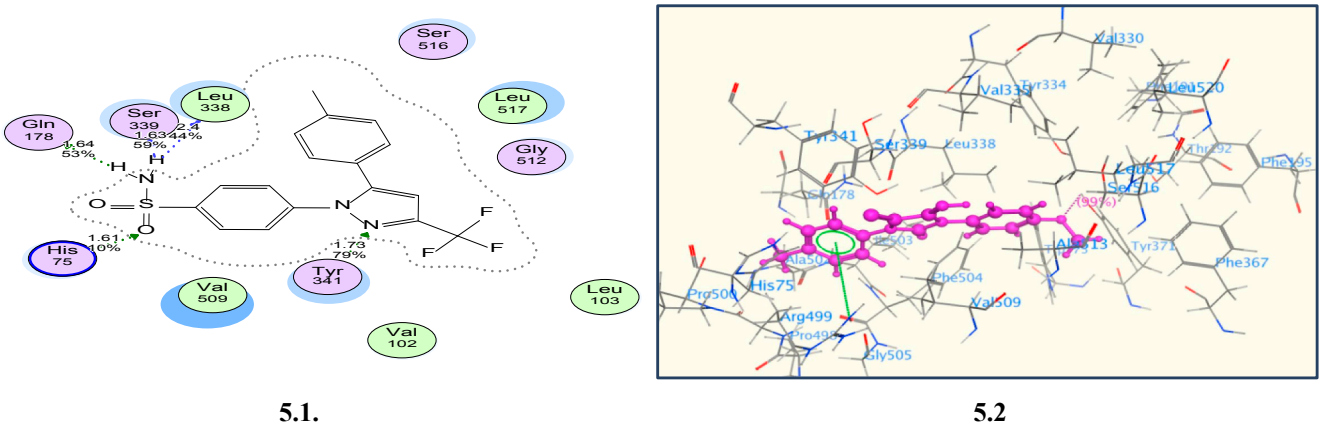

5.1. **5.2**

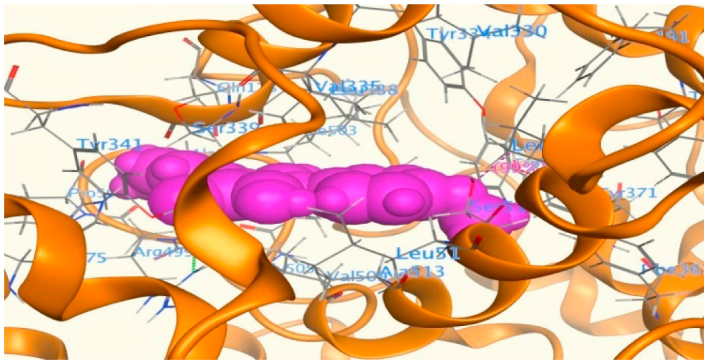

5.3.

Fig. 5. 5.1: 2D binding mode and residues involved in the recognition of celecoxib, **5.2:** 2D binding mode and residues involved in the recognition of compound **2b**, **5.3:** The aligned conformation of **2b** (space filled pink) occupying COX2 binding pocket.

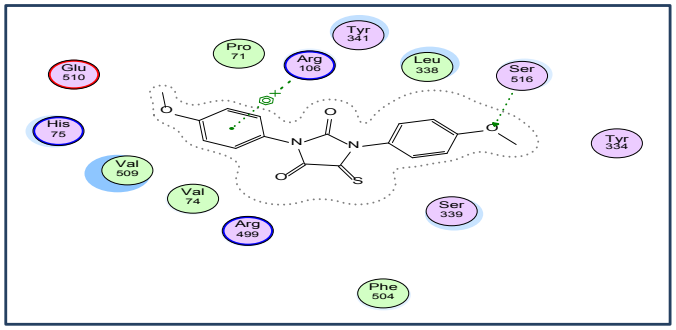

6.1.

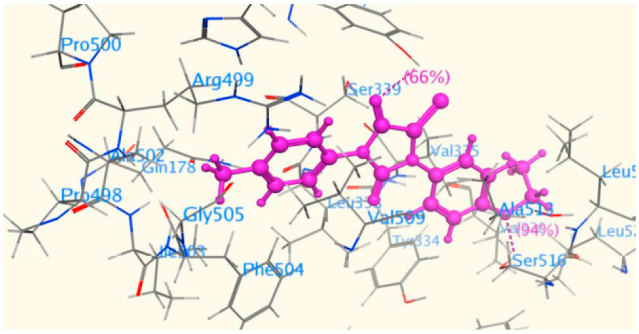

6.2

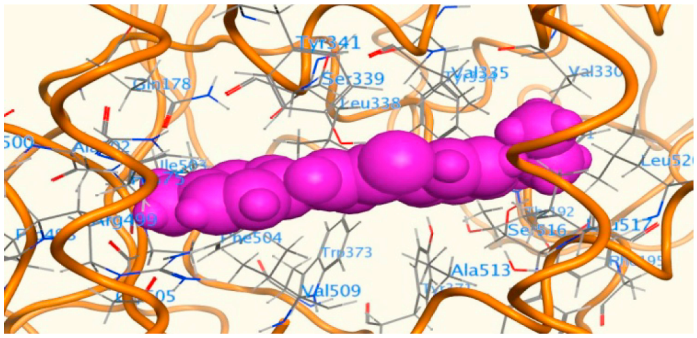

6.3.

Fig. 6. 6.1: 2D binding mode and residues involved in the recognition of compound **3e**, **6.2**: 3D binding mode and residues involved in the recognition of compound **3g**, **6.3**: The aligned conformation of the most active compound **3g** (space filled violet) occupying COX2 binding pocket.

J = 8.7 Hz, Ar-H), 7.49 (d, 2H, *J* = 8.7 Hz, Ar-H), 9.55 (br, 1H, NH), ^{13}C NMR ($CDCl_3$, 100 MHz): 15.7 (CH_3), 21.4 (CH_3), 126.7 (2CH), 126.8 (2CH), 127.0 (2CH), 128.8 (C), 130.1 (C), 130.2 (2CH), 139.6 (C), 140.0 (C), 153.8 (C═N), 154.2 (C═O), 181.6 (C═S); Anal. calcd for $C_{17}H_{15}N_3OS_2$ (341.45): C, 59.80; H, 4.43; N, 12.31; Found: C, 59.76; H, 4.41; N, 12.27%

4.1.4. 4-Imino-1-(4-methoxyphenyl)-5-thioxo-3-(p-tolyl)imidazolidin-2-one (2d)

Yield 78%; m.p. 138–139 °C; IR: ν/cm^{-1}: 3461 (NH), 1777 (C═O), 1667 (C═N), 1252 (C–O), 1173 (C–O), 1128 (C═S); ^{1}H NMR ($CDCl_3$, 400 MHz) δ/ppm = 2.40 (s, 3H, CH_3); 3.85 (s, 3H, OCH_3), 7.04 (d, 2H, *J* = 9.0 Hz, Ar-H), 7.32 (d, 2H, *J* = 8.5 Hz, Ar-H), 7.38 (d, 2H, *J* = 9.0 Hz, Ar-H), 7.43 (d, 2H, *J* = 8.5 Hz, Ar-H), 9.52 (br, 1H, NH), ^{13}C NMR ($CDCl_3$, 100 MHz): 21.2 (CH_3), 55.5 (CH_3), 114.7 (2CH), 125.3 (C), 126.3 (2CH), 128.3 (2CH), 129.3 (C), 130.0 (2CH), 138.7 (C), 154.0 (C═N), 154.4 (C═O), 160.2 (C–O), 181.8 (C═S); Anal. calcd for $C_{17}H_{15}N_3O_2S$ (325.38): C, 62.75; H, 4.65; N, 12.91; Found: C, 62.68; H, 4.61; N, 12.87%

4.1.5. 4-Imino-1,3-bis(4-methoxyphenyl)-5-thioxoimidazolidin-2-one (2e)

Yield 75%; m.p. 118–119 °C; IR: ν/cm^{-1}: 3439 (NH), 1778 (C═O), 1661 (C═N), 1254 (C–O), 1171 (C–O), 1126 (C═S); ^{1}H NMR ($CDCl_3$, 400 MHz) δ/ppm = 3.85 (s, 3H, OCH_3); 3.87 (s, 3H, OCH_3), 7.03 (d, 2H, *J* = 9.1 Hz, Ar-H), 7.05 (d, 2H, *J* = 9.0 Hz, Ar-H), 7.39 (d, 2H, *J* = 9.0 Hz, Ar-H), 7.46 (d, 2H, *J* = 9.1 Hz, Ar-H), 9.50 (br, 1H, NH), ^{13}C NMR ($CDCl_3$, 100 MHz): 55.5 (CH_3), 114.6 (2CH), 114.7 (2CH), 124.2 (C), 125.3 (C), 127.9 (2CH), 128.3 (2CH), 154.1 (C═N), 154.5 (C═O), 159.5 (C–O), 160.2 (C–O), 181.6 (C═S); Anal. calcd for $C_{17}H_{15}N_3O_3S$ (341.38): C, 59.81; H, 4.43; N, 12.31; Found: C, 59.78; H, 4.41; N, 12.34%

4.1.6. 4-Imino-1-(4-methoxyphenyl)-3-(4-(methylthio)phenyl)-5-thioxoimidazolidin-2-one (2f)

Yield 82%; m.p. 125–126 °C; IR: ν/cm^{-1}: 3449 (NH), 1771 (C═O), 1665 (C═N), 1173 (C–O), 1126 (C–O), 1092 (C═S); ^{1}H NMR ($CDCl_3$, 400 MHz) δ/ppm = 2.51 (s, 3H, SCH_3), 3.87 (s, 3H, OCH_3), 7.05 (d, 2H, *J* = 9.0 Hz, Ar-H), 7.40–7.36 (m, 4H, Ar-H), 7.49 (d, 2H, *J* = 8.8 Hz, Ar-H), 9.55 (br, 1H, NH); ^{13}C NMR ($CDCl_3$, 100 MHz): 15.7 (CH_3), 55.5 (CH_3), 114.7 (2CH), 125.2 (C), 126.7 (2CH), 127.0 (2CH), 128.3 (2CH), 128.8 (C), 139.6 (C), 153.9 (C═N), 154.2 (C═O), 160.2 (C–O), 181.7 (C═S); Anal. calcd for $C_{17}H_{15}N_3O_2S_2$ (357.45): C, 57.12; H, 4.23; N, 11.76; Found: C, 57.07; H, 4.21; N, 11.81%

4.1.7. 1-(4-Ethoxyphenyl)-4-imino-5-thioxo-3-(p-tolyl)imidazolidin-2-one (2 g)

Yield 85%; m.p. 157–158 °C; IR: ν/cm^{-1}: 3437 (NH), 1778 (C═O), 1667 (C═N), 1263 (C–O), 1175 (C–O), 1121 (C═S); ^{1}H NMR ($CDCl_3$, 400 MHz) δ/ppm = 1.44 (t, 3H, *J* = 7.0 Hz,$OCH_2\underline{CH_3}$), 2.40 (s, 3H, CH_3), 4.08 (q, *J* = 7.0 Hz, 2H, $O\underline{CH_2}CH_3$), 7.02 (d, 2H, *J* = 9.0 Hz, Ar-H), 7.32 (d, 2H, *J* = 8.1 Hz, Ar-H), 7.37 (d, 2H, *J* = 9.0 Hz, Ar-H), 7.43 (d, 2H, *J* = 8.1 Hz, Ar-H), 9.52 (br, 1H, NH); ^{13}C NMR ($CDCl_3$, 100 MHz): 14.7 (CH_3), 21.2 (CH_3), 63.8 (CH_2), 115.1 (2CH), 125.1 (C), 126.3 (2CH), 128.3 (2CH), 129.4 (C), 130.0 (2CH), 138.7 (C), 154.0 (C═N), 154.4 (C═O), 159.6 (C–O), 181.8 (C═S); Anal. calcd for $C_{18}H_{17}N_3O_2S$ (339.41): C, 63.70; H, 5.05; N, 12.38; Found: C, 63.68; H, 5.07; N, 12.41%.

4.1.8. 1-(4-Ethoxyphenyl)-4-imino-3-(4-methoxyphenyl)-5-thioxoimidazolidin-2-one (2 h)

Yield 90%; m.p. 124–125 °C; IR: ν/cm^{-1}: 3441 (NH), 1777 (C═O), 1667 (C═N), 1254 (C–O), 1173 (C–O), 1125 (C═S); ^{1}H NMR ($CDCl_3$, 400 MHz) δ/ppm = 1.46 (t, 3H, *J* = 7.1 Hz, $OCH_2\underline{CH_3}$), 3.84 (s, 3H, OCH_3), 4.09 (q, 2H, *J* = 7.1 Hz, $O\underline{CH_2}CH_3$), 7.06–7.00 (m, 4H, Ar-H), 7.37 (d, 2H, *J* = 9.0 Hz, Ar-H), 7.46 (d, 2H, *J* = 9.0 Hz, Ar-H), 9.49 (br, 1H, NH); ^{13}C NMR ($CDCl_3$, 100 MHz): 14.7 (CH_3), 55.5 (CH_3), 63.8

(CH_2),114.7 (2CH), 115.1 (2CH), 124.1 (C), 124.5 (C), 128.3 (2CH), 128.9 (2CH), 154.1 (C═N), 154.5 (C═O), 159.5 (C−O), 159.6 (C−O), 181.8 (C═S); Anal. calcd for $C_{18}H_{17}N_3O_3S$ (355.41): C, 60.83; H, 4.82; N, 11.82; Found: C, 60.79; H, 4.80; N, 11.84%.

4.1.9. 1-(4-Ethoxyphenyl)-4-imino-3-(4-(methylthio)phenyl)-5-thioxoimidazolidin-2-one (2i)

Yield 85%; m.p. 128–130 °C; IR: ν/cm^{-1}: 3430 (NH), 1778 (C═O), 1665 (C═N), 1177 (C−O), 1130 (C−O), 1092 (C═S); ^{1}H NMR (DMSO, 400 MHz) δ/ppm = 1.35 (t, 3H, J = 7.1 Hz, $OCH_2\underline{CH_3}$), 2.52 (s, 3H, SCH_3), 4.05 (q, 2H, J = 7.1 Hz, $O\underline{CH_2}CH_3$), 7.08 (d, 2H, J = 9.0 Hz, Ar-H), 7.45–7.38 (m, 4H, Ar-H), 7.49 (d, 2H, J = 8.8 Hz, Ar-H), 9.61 (br, 1H, NH); ^{13}C NMR (DMSO, 100 MHz): 14.7 (CH_3), 14.8 (CH_3), 63.7 (CH_2), 115.0 (2CH), 125.9 (C), 126.2 (2CH), 127.9 (2CH), 129.1 (2CH), 129.5 (C), 138.8 (C), 154.1 (C═N), 154.5 (C═O), 159.2 (C−O), 183.3 (C═S); Anal. calcd for $C_{18}H_{17}N_3O_2S_2$ (371.48): C, 58.20; H, 4.61; N, 11.31; Found: C, 58.17; H, 4.58; N, 11.36%.

4.2. Synthesis of imidazolidin-2,4-diones 3a-i

Each one of imidazolidineiminothione derivatives **2a-i** (0.01 mol) was dissolved in boiling ethanol (20 mL) and treated with dil. HCl (1:1 M ratio). The obtained products were filtered off, washed with cold water, air-dried, and recrystallized from chloroform/*n*-hexane to give the corresponding diones **3a-i**.

4.2.1. 5-Thioxo-1,3-di-p-tolylimidazolidine-2,4-dione (3a)

Yield 75%; m.p. 142–143 °C; IR: ν/cm^{-1}: 1748 (C═O), 1120 (C═S); ^{1}H NMR ($CDCl_3$, 400 MHz) δ/ppm = 2.41 (s, 3H, CH_3), 2.43 (s, 3H, CH_3), 7.42–7.29 (m, 8H, Ar-H); ^{13}C NMR ($CDCl_3$, 100 MHz): 21.2 (CH_3), 21.3 (CH_3),125.6 (2CH), 126.9 (2CH), 127.7 (C), 129.5 (C), 130.1 (2CH), 130.2 (2CH), 139.3 (C), 140.1 (C), 153.0 (C═O), 153.3 (C═O), 182.6 (C═S); Anal. calcd for $C_{17}H_{14}N_2O_2S$ (310.37): C, 65.79; H, 4.55; N, 9.03; Found: C, 65.81; H, 4.53; N, 8.92%.

4.2.2. 3-(4-Methoxyphenyl)-5-thioxo-1-(p-tolyl)imidazolidine-2,4-dione (3b)

Yield 77%; m.p. 164–165 °C; IR: ν/cm^{-1}: 1748 (C═O), 1263 (C−O), 1159 (C−O), 1124 (C═S); ^{1}H NMR ($CDCl_3$, 400 MHz) δ/ppm = 2.43 (s, 3H, CH_3), 3.85 (s, 3H, OCH_3), 7.02 (d, 2H, J = 9.1 Hz, Ar-H),7.31 (d, 2H, J = 8.6 Hz, Ar-H), 7.35 (d, 2H, J = 8.6 Hz, Ar-H), 7.41 (d, 2H, J = 9.1 Hz, Ar-H); ^{13}C NMR ($CDCl_3$, 100 MHz): 21.3 (CH_3), 55.5 (CH_3), 114.7 (2CH), 122.9 (C), 126.9 (2CH), 127.2 (2CH), 129.5 (C), 130.2 (2CH), 140.1 (C), 153.1 (C═O), 153.4 (C═O), 159.5 (C−O), 182.6 (C═S); Anal. calcd for $C_{17}H_{14}N_2O_3S$ (326.37): C, 62.56; H, 4.32; N, 8.58; Found: C, 62.62; H, 4.29; N, 8.62%.

4.2.3. 3-(4-(Methylthio)phenyl)-5-thioxo-1-p-tolylimidazolidine-2,4-dione (3c)

Yield 80%; m.p. 202–203 °C; IR: ν/cm^{-1}: 1760 (C═O); ^{1}H NMR ($CDCl_3$, 400 MHz) δ/ppm = 2.41 (s, 3H, CH_3); 2.53 (s, 3H, SCH_3), 7.32–7.34 (m, 4H, Ar-H), 7.37 (d, 2H, J = 8.6 Hz, Ar-H), 7.51 (d, 2H, J = 8.6 Hz, Ar-H); ^{13}C NMR ($CDCl_3$, 100 MHz): 15.8 (CH_3), 21.3 (CH_3), 126.4 (2CH), 126.9 (2CH), 127.1 (2CH), 128.7 (C), 130.1 (C), 130.2 (2CH), 139.4 (C), 140.0 (C), 153.9 (C═N), 154.2 (C═O), 181.9 (C═S); Anal. calcd for $C_{17}H_{14}N_2O_2S_2$ (342.44): C, 59.63; H, 4.12; N, 8.18; Found: C, 59.52; H, 4.07; N, 8.23.

4.2.4. 1-(4-Methoxyphenyl)-5-thioxo-3-p-tolylimidazolidine-2,4-dione (3d)

Yield 78%; m.p. 153–154 °C; IR: ν/cm^{-1}: 1777, 1667 (C═O); ^{1}H NMR ($CDCl_3$, 400 MHz) δ/ppm = 2.42 (s, 3H, CH_3); 3.91 (s, 3H, OCH_3), 7.11 (d, 2H, J = 8.8 Hz, Ar-H), 7.30 (d, 2H, J = 8.7 Hz, Ar-H), 7.42 (d, 2H, J = 9.0 Hz, Ar-H), 7.47 (d, 2H, J = 8.6 Hz, Ar-H); ^{13}C NMR ($CDCl_3$, 100 MHz): 21.3 (CH_3), 55.4 (CH_3), 114.8 (2CH), 125.2 (C), 126.7 (2CH), 128.2 (2CH), 129.4 (C), 130.1 (2CH), 138.8 (C), 154.2, 154.6, 160.2, 181.8 (C═S); Anal. calcd for $C_{17}H_{14}N_2O_3S$(326.37): C, 62.56; H, 4.32; N, 8.58; Found: C, 62.48; H, 4.29; N, 8.64.

4.2.5. 1,3-Bis(4-methoxyphenyl)-5-thioxoimidazolidine-2,4-dione (3e)

Yield 80%; m.p. 181–182 °C; IR: ν/cm^{-1}: 1746 (C═O), 1254 (C−O), 1161 (C−O), 1120 (C═S); ^{1}H NMR ($CDCl_3$, 400 MHz) δ/ppm = 3.85 (s, 3H, OCH_3), 3.86 (s, 3H, OCH_3), 7.07–7.00 (m, 4H, Ar-H), 7.35 (d, 2H, J = 9.1 Hz, Ar-H), 7.40 (d, 2H, J = 9.1 Hz, Ar-H); ^{13}C NMR ($CDCl_3$, 100 MHz): 55.5 (CH_3), 56.2 (CH_3),114.7 (2CH), 114.8 (2CH), 122.9 (C), 124.6 (C), 127.2 (2CH), 128.4 (2CH), 153.1 (C═O), 153.6 (C═O), 159.9 (C−O), 160.3 (C−O), 182.8 (C═S); Anal. calcd for $C_{17}H_{14}N_2O_4S$ (342.37): C, 59.64; H, 4.12; N, 8.18; Found: C, 59.66; H, 4.07; N, 8.23%.

4.2.6. 1-(4-Methoxyphenyl)-3-(4-(methylthio)phenyl)-5-thioxoimidazolidine-2,4-dione (3f)

Yield 75%; m.p. 162–163 °C; IR: ν/cm^{-1}: 1744 (C═O), 1173 (C−O), 1163 (C−O), 1094 (C═S); ^{1}H NMR ($CDCl_3$, 400 MHz) δ/ppm = 2.52 (s, 3H, SCH_3), 3.88 (s, 3H, OCH_3), 7.04 (d, 2H, J = 9.0 Hz, Ar-H), 7.39–7.31 (m, 4H, Ar-H), 7.42 (d, 2H, J = 8.8 Hz, Ar-H), ^{13}C NMR ($CDCl_3$, 100 MHz): 15.5 (CH_3), 55.6 (CH_3), 114.8 (2CH), 124.5 (C), 126.0 (2CH), 126.8 (2CH), 127.1 (C), 128.4 (2CH), 140.4 (C), 152.8 (C═O), 153.3 (C═O), 160.4 (C−O), 182.5 (C═S); Anal. calcd for $C_{17}H_{14}N_2O_3S_2$ (358.43): C, 56.96; H, 3.94; N, 7.82; Found: C, 57.04; H, 3.97; N, 7.86%.

4.2.7. 1-(4-Ethoxyphenyl)-5-thioxo-3-(p-tolyl)imidazolidine-2,4-dione (3 g)

Yield 77%; m.p. 159–160 °C; IR: ν/cm^{-1}: 1750 (C═O), 1260 (C−O), 1159 (C−O), 1116 (C═S); ^{1}H NMR ($CDCl_3$, 400 MHz) δ/ppm = 1.39 (t, 3H, J = 7.0 Hz, $OCH_2\underline{CH_3}$), 2.41 (s, 3H, CH_3), 4.10 (q, 2H, J = 7.0 Hz, $O\underline{CH_2}CH_3$), 7.03 (d, 2H, J = 9.0 Hz, Ar-H), 7.40–7.29 (m, 6H, Ar-H), ^{13}C NMR ($CDCl_3$, 100 MHz): 14.7 (CH_3), 21.2 (CH_3), 63.8 (CH_2), 115.3 (2CH), 124.4 (C), 125.6 (2CH), 127.8 (C), 128.3 (2CH), 130.1 (2CH), 139.2 (C), 153.0 (C═O), 153.5 (C═O), 159.8 (C−O), 182.7 (C═S); Anal. calcd for $C_{18}H_{16}N_2O_3S$ (340.40): C, 63.51; H, 4.74; N, 8.23; Found: C, 63.47; H, 4.76; N, 8.27%.

4.2.8. 1-(4-Ethoxyphenyl)-3-(4-methoxyphenyl)-5-thioxoimidazolidine-2,4-dione (3 h)

Yield 80%; m.p. 134–135 °C; IR: ν/cm^{-1}: 1746 (C═O), 1254 (C−O), 1161 (C−O), 1125 (C═S); ^{1}H NMR ($CDCl_3$, 400 MHz) δ/ppm = 1.44 (t, 3H, J = 7.0 Hz, $OCH_2\underline{CH_3}$), 3.85 (s, 3H, OCH_3), 4.07 (q, 2H, J = 7.0 Hz, $O\underline{CH_2}CH_3$), 7.05–7.00 (m, 4H, Ar-H), 7.34 (d, 2H, J = 9.1 Hz, Ar-H), 7.41 (d, 2H, J = 9.1 Hz, Ar-H); ^{13}C NMR ($CDCl_3$, 100 MHz): 14.7 (CH_3), 55.6 (CH_3), 63.9 (CH_2), 114.7 (2CH), 115.3 (2CH), 122.9 (C), 124.4 (C), 127.2 (2CH), 128.3 (2CH), 153.1 (C═O), 153.6 (C═O), 159.8 (C−O), 159.9 (C−O), 182.8 (C═S); Anal. calcd for $C_{18}H_{16}N_2O_4S$ (356.40): C, 60.66; H, 4.53; N, 7.86; Found: C, 60.74; H, 4.51; N, 7.93%.

4.2.9. 1-(4-Ethoxyphenyl)-3-(4-(methylthio)phenyl)-5-thioxoimidazolidine-2,4-dione (3i)

Yield 85%; m.p. 108–109 °C; IR: ν/cm^{-1}: 1746 (C═O), 1252 (C−O), 1153 (C−O), 1115 (C═S); ^{1}H NMR (DMSO, 400 MHz) δ/ppm = 1.35 (t, 3H, J = 7.0 Hz, $OCH_2\underline{CH_3}$), 2.52 (s, 3H, SCH_3), 4.09 (q, 2H, J = 7.0 Hz, $O\underline{CH_2}CH_3$), 7.09 (d, 2H, J = 9.0 Hz, Ar-H), 7.40 (d, 2H, J = 9.0 Hz, Ar-H), 7.46–7.43 (m, 4H, Ar-H); ^{13}C NMR (DMSO, 100 MHz): 14.7 (CH_3), 14.8 (CH_3), 63.8 (CH_2), 115.1 (2CH), 125.3 (C), 126.3 (2CH), 127.4 (2CH), 127.7 (C), 129.1 (2CH), 139.7 (C), 153.7 (C═O), 154.0 (C═O), 159.2 (C−O), 185.2 (C═S); Anal. calcd for $C_{18}H_{16}N_2O_3S_2$ (372.46): C, 58.04; H, 4.33; N, 7.52; Found: C, 57.97; H, 4.29; N, 7.48%.

4.3. Biological evaluation

4.3.1. Antiinflammatory screening

Male Sprague Dawley rats weighing 250 g were purchased from local source and kept at room temperature (22 ± 2 °C) in a light-controlled room with an alternating 12 h light/dark cycle. They were fasted with free access to water at least 16 h prior to experiments. The tested compounds were prepared as suspension in vehicle (0.5% methyl cellulose) and celecoxib was used as a standard drug. The positive control group animals received the reference drug while the negative control received only the vehicle. The anti-inflammatory activity was evaluated using *in vivo* rat carrageenan-induced foot paw edema model reported previously [21,22]. Edema was produced by injecting 0.25 mL of a solution of 1% l-carrageenan in the hind paw. The rats were injected intraperitoneally with 1 mL suspension in 0.5% methyl cellulose of the tested compounds and reference drug. The percentage edema (E%) at each time point and the percentage inhibition of edema (I%) of each group were calculated as follows

$$\text{Oedema(E\%)} = \frac{PT_t PT_0}{PT_0} \text{Inhibition(\%)} = \left(1 - \frac{E_D}{E_C}\right) \times 100$$

Where, PT_0 and PT_t are the paw thickness (mm) before and after carrageenan injection, respectively. The E_D and E_C are the mean percentage edema of the treated and control groups, respectively. Values reported as mean ± S.E.M., significant differences were calculated using ANOVA.

4.3.2. In vitro cyclooxygenase inhibitory assay

The *in vitro* ability of test compounds and celecoxib to inhibit the COX-1 and COX-2 isozymes was carried out using Cayman colorimetric COX (ovine) inhibitor screening assay kit (Catalog no. 701070) supplied by Cayman chemicals, USA. The calculations were performed as per the kit guidelines [21–23].

4.3.3. Determination of the IC_{50} of the target compounds

IC_{50} (Concentration at which there was 50% inhibition of COX-1) of the target compounds were determined by the aid of Cayman colorimetric COX (ovine) inhibitor screening assay kit through the determination of the average absorbance of all the samples. Subtract the absorbance of the background wells from the Initial Activity sample, then divide by the 100% Initial Activity sample, and multiply by 100 to give the percent inhibition. Graph the percent inhibition and determine the IC_{50} value by using the three results obtained.

4.3.4. Analgesic activity

Male albino Swiss mice (25 g body weight) were divided into groups (N = a). Each mouse was initially placed on a hot plate thermostatically maintained at 58 °C [26]. The mouse was watched carefully for the time in seconds in which it displays nociceptive responses exhibited as licking or blowing (fanning) its front paws. This time was considered as the control reaction time. A cut-off time of 60 s was used to avoid damage to the paws. To test the analgesic activity of the compounds each group of mice was treated with one dose of the test compounds (5–200 μM/Kg ip). The reaction time was then retested at 30, 60 and 120 min after injection (each animal acted as its own control). The percentage changes in the reaction were then calculated. The ED_{50} for each compound was then calculated by linear regression.

4.3.5. Molecular modelling

Two different Cox target enzymes were investigated. These include ovine COX-1 complexed with celecoxib (PDB code: 3kk6) [27] and COX-2 complexed with a selective inhibitor, (celecoxib (PDB code: 3LN1) [28]. Those were retrieved from the Protein Data Bank, http://www.rcsb.org/pdb/home/home.do. For each docking target, all hydrogens were added then water molecules were removed from the surface of the protein. The enzyme structure was subjected to a refinement protocol in which the constraints on the enzyme were gradually removed and minimized until the Root mean square deviation (RMSD) gradient was 0.01 kcal/mol Å. The energy minimization (EM) was carried out using the molecular mechanics force field 'AMBER.' The energy-minimized structure was used for molecular dynamics studies. For each compound, EM were performed using 1000 steps of steepest descent, followed by conjugate gradient minimization to a RMSD energy gradient of 0.01 kcal/mol Å. The active site of each enzyme was defined using a radius of 10.0 Å around celewcoxib. Energy of binding was calculated as the difference between the energy of the complex and individual energies of the enzyme and ligand [29–32].

Appendix A. Supplementary material

Supplementary data to this article can be found online at https://doi.org/10.1016/j.bioorg.2019.03.075.

References

[1] M. Kaur, M. Singh, O. Silakari, Eur. J. Med. Chem. 67 (2013) 434–446.
[2] G.Y. Chen, G. Nunez, Nat. Rev. Immunol. 10 (2010) 826–837.
[3] M.B. Goldring, M. Otero, Curr. Opin. Rheumatol. 23 (2011) 471–478.
[4] N. Herrmann, S.A. Chau, I. Kircanski, K.L. Lanctot, Drugs 71 (2011) 2031–2065.
[5] B. Sever, M.D. Altıntop, G. Kus, M. Ozkurt, A. Ozdemir, Z.A. Kaplanckl, Eur. J. Med. Chem. 113 (2016) 179–186.
[6] J. Grover, V. Kumar, V. Singh, K. Bairwa, M.E. Sobhia, S.M. Jachak, Eur. J. Med. Chem. 80 (2014) 47–56.
[7] R. Aggarwal, A. Bansal, I. Rozas, B. Kelly, P. Kaushik, D. Kaushik, Eur. J. Med. Chem. 70 (2013) 350–357.
[8] S. Chennamaneni, B. Zhong, R. Lama, B. Su, Eur. J. Med. Chem. 56 (2012) 17–29.
[9] M. Madhukar, S. Sawraj, P.D. Sharma, Eur. J. Med. Chem. 45 (2010) 2591–2596.
[10] A.A. Farag, M.F. El Shehry, S.Y. Abbas, S.N. Abd-Alrahman, A.A. Atrees, H.Z. Albasheer, Y.A. Ammar, Z. Naturforsch, B 70 (2015) 519–526.
[11] C. Congiu, M.T. Cocco, V. Onnis, Bioorg Med Chem Lett 18 (2008) 989–993.
[12] I.R. Siddiqui, P.K. Singh, V. Srivastava, J. Singh, Indian J. Chem. 49B (2010) 512–520.
[13] Y.I. Lin, P.J. Peterson, Y. Yang, W.J. Weiss, D.M. Shales, et al., Bioorg. Med. Chem. Lett. 16 (2008) 1890–1902.
[14] P. Molina, A. Tárraga, F. Otón, Org. Biomol. Chem. 10 (2012) 1711–1724.
[15] Z. Jin, Nat. Prod. Rep. 30 (2013) 869–915.
[16] Y.A. Ammar, M.A.M.Sh. El-Sharief, M.M. Ghorab, Y.A. Mohamed, A. Ragab, S.Y. Abbas, Cur. Org. Syn. 13 (2016) 466–475.
[17] Z. Moussa, M.A.M.S. El-Sharief, S.Y. Abbas, Eur. J. Med. Chem. 122 (2016) 419–428.
[18] M.A.M.Sh. El-Sharief, S.Y. Abbas, M.A. Zahran, Y.A. Mohamed, A. Ragab, Y.A. Ammar, Z. Naturforsch, B 71 (2016) 875–881.
[19] Y.A. Ammar, S.Y. Abbas, M.A.M.Sh. El-Sharief, M.A. Salem, A. Ragab, Eur. J. Chem. 8 (2017) 76–81.
[20] M.A.M.Sh. El-Sharief, S.Y. Abbas, Z. Moussa, E.W. El-Gammal, A.M.Sh. El-Sharief, Croat. Chem. Acta. 91 (3) (2018) 1–6.
[21] C.A. Winter, E.A. Risely, G.W. Nuss, Proc. Soc. Exper. Biol. Med. 111 (1962) 544–547.
[22] S.H. Lee, M.J. Son, H.K. Ju, C.X. Lin, T.C. Moon, H.G. Choi, J.K. Son, H.W. Chang, Biol. Pharma. Bulletin 27 (2004) 786–788.
[23] E. Manivannan, S.C. Chaturvedi, Bioorg. Med. Chem. 19 (2011) 4520–4528.
[24] R. Maccari, M.L. Barreca, G. Bruno, A. Rotondo, A. Rossi, G. Chiricosta, R.D. Paola, L. Sautebin, S. Cuzzocread, M.G. Vigorita, R. Ottana, Biol. Med. Chem 13 (2005) 4243.
[25] J.K. Gierse, J.J. McDonald, S.D. Hauser, S.H. Rangwala, C.M. Kobolt, K.J. Seibert, Biol. Chem. 271 (1996) 15.
[26] G.E. Leighton, M.A. Johnson, K.G. Meecham, R.G. Hill, J. Hughes, British J. Pharm. 92 (1987) 915–922.
[27] G. Rimon, R.S. Sidhu, D.A. Lauver, J.Y. Lee, N.P. Sharma, C. Yuan, R.A. Frieler, R.C. Trievel, B.R. Lucchesi, W.L. Smith, Proc. Natl. Acad. Sci. 107 (2010) 28–33.
[28] J.L. Wang, D. Limburg, M.J. Graneto, J. Springer, J.R. Hamper, S. Liao, J.L. Pawlitz, R.G. Kurumbail, T. Maziasz, J.J. Talley, J.R. Kiefer, J. Carter, Bioorg. Med. Chem. Lett. 20 (2010) 7159–7163.
[29] S. Profeta, N.L. Allinger, J. Am. Chem. Soc. 107 (1985) 1907–1918.
[30] N.L. Allinger, Conformational analysis. 130. MM2, J. Am. Chem. Soc. 99 (1977) 8127–8134.
[31] P. Labute, C. Williams, M. Feher, E. Sourial, J.M. Schmidt, Flexible alignment of small molecules, J. Med. Chem. 44 (2001) 1483–1490.
[32] S. Kearsley, G.M. Smith, Tetrahedron Comput. Methodol. 3 (1990) 615–633.